AIP | Advances

Giant fifth-order nonlinearity via tunneling induced quantum interference in triple quantum dots

Si-Cong Tian, Ren-Gang Wan, Cun-Zhu Tong, and Yong-Qiang Ning

Citation: AIP Advances **5**, 027111 (2015); doi: 10.1063/1.4908008
View online: http://dx.doi.org/10.1063/1.4908008
View Table of Contents: http://scitation.aip.org/content/aip/journal/adva/5/2?ver=pdfcov
Published by the AIP Publishing

AIP ADVANCES **5**, 027111 (2015)

Giant fifth-order nonlinearity via tunneling induced quantum interference in triple quantum dots

Si-Cong Tian,[1,a] Ren-Gang Wan,[2] Cun-Zhu Tong,[1,b] and Yong-Qiang Ning[1]
[1]*State Key laboratory of Luminescence and Applications, Changchun Institute of Optics, Fine Mechanics and Physics, Chinese Academy of Sciences, Changchun 130033, China*
[2]*School of Physics and Information Technology, Shaanxi Normal University, Xi'an 710062, China*

(Received 8 December 2014; accepted 2 February 2015; published online 9 February 2015)

Schemes for giant fifth-order nonlinearity via tunneling in both linear and triangular triple quantum dots are proposed. In both configurations, the real part of the fifth-order nonlinearity can be greatly enhanced, and simultaneously the absorption is suppressed. The analytical expression and the dressed states of the system show that the two tunnelings between the neighboring quantum dots can induce quantum interference, resulting in the giant higher-order nonlinearity. The scheme proposed here may have important applications in quantum information processing at low light level. [http://dx.doi.org/10.1063/1.4908008]

I. INTRODUCTION

Nonlinear optical interactions have been extensively studied because of their potential applications in optical technology and quantum information applications.[1] Obtaining large nonlinear interaction at a low light level is one of the important goals.[2,3] For the susceptibility magnitude decreases typically with increasing order of nonlinearity, most nonlinear studies at low light level have focused on the third-order processes.[4–9] In these studies, enhanced third-order nonlinearity and suppressed linear absorption can be obtained, with the help of electromagnetically induced transparency (EIT).[10] Despite the success of third-order nonlinearity, some fundamental studies and applications require or can benefit from large fifth-order nonlinearities. There are mainly two methods for studying fifth-order nonlinearity, one is based on minimizing cascaded contributions,[11,12] and the other is by means of the interaction of cascaded nonlinearities.[13,14] Understanding the mechanism of fifth-order nonlinearity, especially with the ability to control it, can have broad impacts in many fields including multiwave mixing[15,16] and optical solitons.[17–19]

On the other hand, quantum dots (QDs) have many advantages over atoms due to its high nonlinear optical coefficients, customized design and ease of integration. Double quantum dots (DQDs) containing two closely spaced QDs can be fabricated by using self assembled dot growth technology.[20] The tunneling of electrons between the dots, which is controlled by an external electric field, can induce quantum interference and coherence.[21–24] Therefore, fundamental studies of DQDs such as EIT and slow light,[25] entanglement,[26] narrowing of fluorescence spectrum,[27] coherent population transfer[28] and enhanced Kerr nonlinearity[29] are investigated. Moreover, triple quantum dots (TQDs) are receiving much attention recently, due to its multilevel structure and extra controlling parameters which cannot be found in DQDs. TQDs composed of linear or triangular type have been fabricated in much experimental progress.[30–33] Theoretical works of both configurations of TQDs such as transmission-dispersion spectrum,[34] multiple transparency windows,[35] resonance fluorescence spectrum,[36] optical switch,[37] Kerr nonlinearity[38] and optical bistability[39] are studied.

[a]Electronic mail: tiansicong@ciomp.ac.cn
[b]Electronic mail: tongcz@ciomp.ac.cn

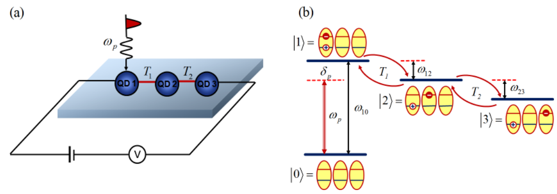

FIG. 1. (a) The schematic of the setup for linear TQDs. (b) The schematic of the energy level for linear TQDs.

Most recently, a scheme for obtaining large fifth-order nonlinearity using DQDs is proposed.[40] The real part of the fifth-order nonlinearity can be increased with vanishing absorption by the competition between the linear and nonlinear susceptibility. In this paper, we propose to use quantum interference induced by the tunneling, to acquire enhanced fifth-order nonlinearity in two different types of TQDs, one is linear, and the other is triangular. With proper parameters, the real part of the fifth-order nonlinearity of both configurations is greatly enhanced compared with DQDs, and simultaneously the absorption is suppressed. An analytical expression and the dressed states of the TQDs show that the two tunnelings between the QDs is responsible for the enhancement of the fifth-order nonlinear response.

II. LINEAR TQDS

We first consider a linear TQDs. The setup of the linear TQDs is shown in Fig. 1(a). Three QDs are arranged linearly by two gate electrodes, which can be used to control the electron tunneling. And V is the bias voltage. One laser field probes QD 1. Fig. 1(b) shows the energy level of the linear TQDs. Here, state $|0\rangle$ denotes the ground state without excitation. State $|1\rangle$ denotes the direct exciton state with one electron-hole pair, exited by the laser field. The electron can tunnel between the neighbor QDs when the gate voltage is on, thus the indirect exciton states are $|2\rangle$ and $|3\rangle$, respectively.

The Hamiltonian with the basis $\{|0\rangle, |1\rangle, |2\rangle, |3\rangle\}$ under the rotating wave and the electric dipole approximations can be written as (assumption of $\hbar = 1$)

$$H_I = \begin{pmatrix} 0 & -\Omega_p & 0 & 0 \\ -\Omega_p & \delta_p & -T_1 & 0 \\ 0 & -T_1 & \delta_p - \omega_{12} & -T_2 \\ 0 & 0 & -T_2 & \delta_p - \omega_{12} - \omega_{23} \end{pmatrix}. \quad (1)$$

Here $\Omega_p = \mu_{01} E_p$ denotes the probe Rabi frequency, with E_p being the electric field amplitude, and $\mu_{01} = \boldsymbol{\mu}_{01} \cdot \mathbf{e}$ being the electric dipole moment of transition $|0\rangle \leftrightarrow |1\rangle$. ($\mathbf{e}$ is the polarization vector.) T_1 and T_2 are the coupling intensities of the two tunnelings, and they relay on the intrinsic sample barrier, as well as the extrinsic electric field. The probe detuning is defined as $\delta_p = \omega_{10} - \omega_p$, where ω_p is the probe frequency, and ω_{10} is the transition frequency of the exited state $|1\rangle$ and ground state $|0\rangle$. ω_{12} and ω_{23} are the energy splittings of the excited states, and they relay on the effective confinement potential manipulated by the external voltage.

The state vector at any time t is

$$|\Psi_I(t)\rangle = a_0(t)|0\rangle + a_1(t)|1\rangle + a_2(t)|2\rangle + a_3(t)|3\rangle, \quad (2)$$

which obeys the Schrödinger equation

$$\frac{d}{dt}|\Psi_I(t)\rangle = -iH_I(t)|\Psi_I(t)\rangle. \quad (3)$$

Substituting Eq. (1) and (2) into Eq. (3), and using the Weisskopf-Wigner theory,[41,42] the dynamical equations for the atomic probability amplitudes in the interaction picture can be obtained:

$$i\dot{a}_0 = -\Omega_p a_1, \quad (4a)$$

$$i\dot{a}_1 = -\Omega_p a_0 - T_1 a_2 + (\delta_p - i\gamma_1) a_1, \quad (4b)$$

$$i\dot{a}_2 = -T_1 a_1 - T_2 a_3 + \left(\delta_p - \omega_{12} - i\gamma_2\right) a_2, \tag{4c}$$

$$i\dot{a}_3 = -T_2 a_2 + \left(\delta_p - \omega_{12} - \omega_{23} - i\gamma_3\right) a_3, \tag{4d}$$

with $|a_0|^2 + |a_1|^2 + |a_2|^2 + |a_3|^2 = 1$. And here $\gamma_i = \frac{1}{2}\Gamma_{i0} + \gamma_{i0}^d$ $(i = 1-3)$ are typical effective decay rates, which are contributed by two parts, radiative decay rate Γ_{i0} from $|i\rangle \to |0\rangle$ and the pure dephasing rate γ_{i0}^d.

It is well known that the polarization of the medium is

$$P = \varepsilon_0 \chi_p E_p = \frac{\Gamma}{V}\mu_{01} a_1 {a_0}^*, \tag{5}$$

where ε_0 is the dielectric constant, Γ is the optical confinement factor and V is the volume of the QDs.[43] From Eq. (5) the probe susceptibility can be obtained, which is given by

$$\chi_p = \frac{\Gamma}{V}\frac{{\mu_{01}}^2}{\varepsilon_0 \hbar \Omega_p} a_1 {a_0}^* = \frac{\Gamma}{V}\frac{{\mu_{01}}^2}{\varepsilon_0 \hbar}\chi. \tag{6}$$

Here χ is independent of Γ and V. So in the following we will focus on the susceptibility χ. In the steady state, we solve Eq. (4) under the weak field approximation $\left(|a_0|^2 = 1\right)$, then

$$\chi = \frac{1}{\Gamma_1 - \frac{{T_1}^2\Gamma_3}{\Gamma_2\Gamma_3 - {T_2}^2}} \cdot \frac{1}{1 + \frac{{\Omega_p}^2}{\left|\Gamma_1 - \frac{{T_1}^2\Gamma_3}{\Gamma_2\Gamma_3 - {T_2}^2}\right|^2}\left(1 + {T_1}^2\frac{|\Gamma_3|^2}{\left|\Gamma_2\Gamma_3 - {T_2}^2\right|^2} + (T_1T_2)^2\frac{1}{\left|\Gamma_2\Gamma_3 - {T_2}^2\right|^2}\right)}. \tag{7}$$

where $\Gamma_1 = \delta_p - i\gamma_1$, $\Gamma_2 = \delta_p - \omega_{12} - i\gamma_2$, $\Gamma_3 = \delta_p - \omega_{12} - \omega_{23} - i\gamma_3$. Using the Maclaurin formula and neglecting the higher-order smaller terms,[40] χ can be expanded into the fourth-order of Ω_p,

$$\chi = \chi^{(1)} + \chi^{(3)}{\Omega_p}^2 + \chi^{(5)}{\Omega_p}^4, \tag{8}$$

where $\chi^{(1)}$, $\chi^{(3)}$ and $\chi^{(5)}$ correspond to the first-order linear, the third-order nonlinear and the fifth-order nonlinear parts of the susceptibility, respectively, and they are given by

$$\chi^{(1)} = \frac{1}{\Gamma_1 - \frac{{T_1}^2\Gamma_3}{\Gamma_2\Gamma_3 - {T_2}^2}}, \tag{9a}$$

$$\chi^{(3)} = -\frac{1}{\Gamma_1 - \frac{{T_1}^2\Gamma_3}{\Gamma_2\Gamma_3 - {T_2}^2}} \cdot \frac{1}{\left|\Gamma_1 - \frac{{T_1}^2\Gamma_3}{\Gamma_2\Gamma_3 - {T_2}^2}\right|^2} \cdot \left(1 + T_1^2\frac{|\Gamma_3|^2}{\left|\Gamma_2\Gamma_3 - {T_2}^2\right|^2} + (T_1T_2)^2\frac{1}{\left|\Gamma_2\Gamma_3 - {T_2}^2\right|^2}\right), \tag{9b}$$

$$\chi^{(5)} = \frac{1}{\Gamma_1 - \frac{{T_1}^2\Gamma_3}{\Gamma_2\Gamma_3 - {T_2}^2}} \cdot \frac{1}{\left|\Gamma_1 - \frac{{T_1}^2\Gamma_3}{\Gamma_2\Gamma_3 - {T_2}^2}\right|^4} \cdot \left(1 + {T_1}^2\frac{|\Gamma_3|^2}{\left|\Gamma_2\Gamma_3 - {T_2}^2\right|^2} + (T_1T_2)^2\frac{1}{\left|\Gamma_2\Gamma_3 - {T_2}^2\right|^2}\right)^2. \tag{9c}$$

According to Eqs. (9a) and (9c), we show the imaginary part of the linear susceptibility $\mathrm{Im}[\chi^{(1)}]$ (dotted line) and the real part of fifth-order nonlinearity $\mathrm{Re}[\chi^{(5)}]$ (solid line) as a function of δ_p in Fig. 2. And in our calculations, the value of the parameters are based on Ref. 38 and references therein, and the values are realistic and scaled by γ_1.

First, with only one tunneling T_1, the system goes to the DQDs.[40] From the imaginary part of the linear susceptibility $\mathrm{Im}[\chi^{(1)}]$ we can acquire one transparency window, within which the real part of the fifth-order nonlinear susceptibility $\mathrm{Re}[\chi^{(5)}]$ is not large, as shown in Fig. 2(a). When both tunnelings T_1 and T_2 are present, the system turns to be a linear TQDs. With zero value of energy splittings ($\omega_{12} = \omega_{23} = 0$), $\mathrm{Im}[\chi^{(1)}]$ is symmetrical with two transparency windows, between which a narrow absorption peak arises. And in the vicinity of the single-photon resonance ($\delta_p = 0$), $\mathrm{Re}[\chi^{(5)}]$ is enhanced about 30 times the magnitude of that in DQDs [Fig. 2(b)].

However, this enhanced $\mathrm{Re}[\chi^{(5)}]$ is accompanied by a strong absorption. Then we increase the energy splitting ω_{23} from 0 to 0.4 and show the corresponding results in Figs. 2(c) and 2(d). The transparency window on the right becomes narrower, while the one on the left becomes wider.

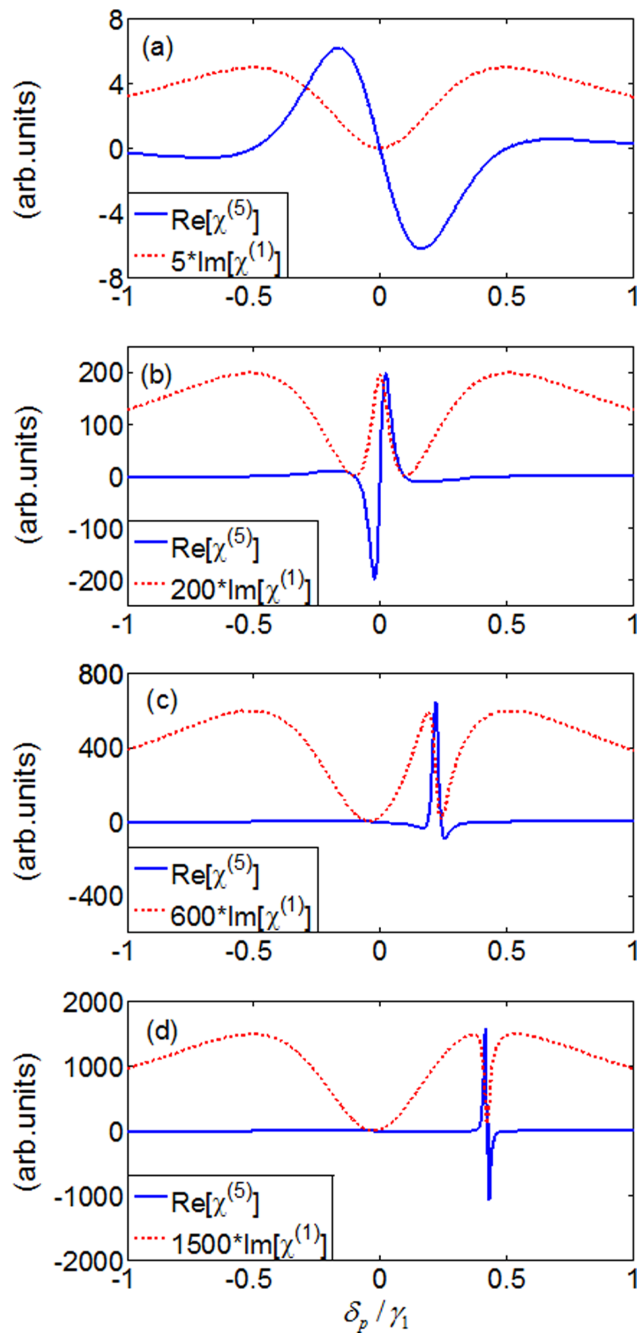

FIG. 2. Variation of the imaginary part of the linear susceptibility Im[$\chi^{(1)}$] (dotted line) and the real part of fifth-order nonlinearity Re[$\chi^{(5)}$] (solid line) as a function of probe detuning δ_p. (a) $T_2 = 0$, $\omega_{23} = 0$. (b) $T_2 = 0.1$, $\omega_{23} = 0$. (c) $T_2 = 0.1$, $\omega_{23} = 0.2$. (d) $T_2 = 0.1$, $\omega_{23} = 0.4$. Other parameters are $T_1 = 0.5$, $\omega_{12} = 0$, $\gamma_1 = 1$, $\gamma_2 = \gamma_3 = 10^{-3}\gamma_1$.

Simultaneously, Re[$\chi^{(5)}$] is greatly enhanced and gradually enters the narrowed transparency window. For instance, when $\omega_{23} = 0.4$, Re[$\chi^{(5)}$] is significantly enhanced by about three orders of magnitude compared with the DQDs [Fig. 2(d)]. The results indicate that one can obtain giant fifth-order nonlinearity with reduced absorption by the tunnelings, and this is useful for applications of low intensity nonlinear optics.

From Eq. (9c), the fifth-order nonlinearity can be separated into two parts, one is proportional to the product of $(T_1T_2)^4$, which we denote as F_1, and the other is independent of the product, which we denote as F_2. Then $\chi^{(5)}$ can be expressed as $\chi^{(5)} = F_1 + F_2$. For comparison, we plot both the

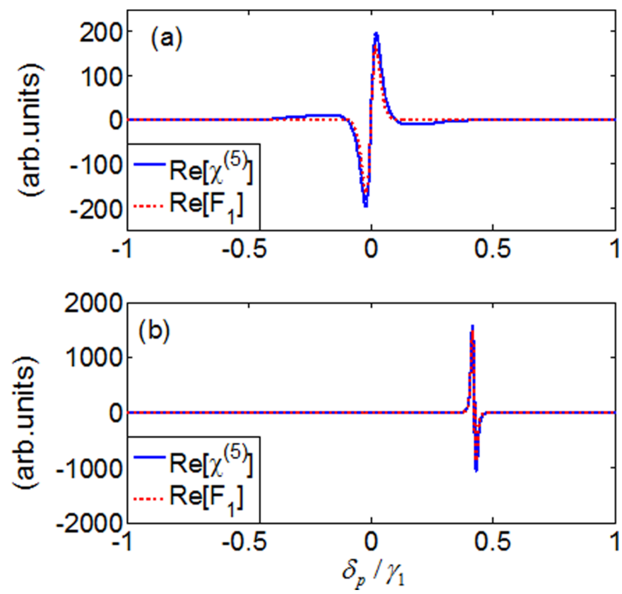

FIG. 3. Variation of Re[F_1] (dotted line) and Re[$\chi^{(5)}$] (solid line) as a function of the probe detuning δ_p. (a) $\omega_{23} = 0$, (b) $\omega_{23} = 0.4$. Other parameters are $T_1 = 0.5$, $T_2 = 0.1$, $\omega_{12} = 0$, $\gamma_1 = 1$, $\gamma_2 = \gamma_3 = 10^{-3}\gamma_1$.

term Re[F_1] and Re[$\chi^{(5)}$] as a function of δ_p in Fig. 3, from which one can see that the profile of Re[$\chi^{(5)}$] is almost the same with Re[F_1]. So the giant enhancement of the real part of fifth-order nonlinearity is originates from the interaction of the two tunnelings T_1 and T_2.

Last we provide the physical interpretation under the dressed state picture. To do that, the Hamiltonian corresponding to the system and the tunneling couplings need to be diagonalized. Then the expressions of the dressed states are

$$|i\rangle = \cos\varphi\cos\theta\,|1\rangle + \sin\varphi\,|2\rangle + \cos\varphi\sin\theta\,|3\rangle \;\; (i = a, b, c), \tag{10}$$

where $\tan\varphi = \frac{\lambda_i(\lambda_i-\omega_{12}-\omega_{23})}{\sqrt{T_2{}^2\lambda_i{}^2+T_1{}^2(\lambda_i-\omega_{12}-\omega_{23})^2}}$ and $\tan\theta = \frac{T_2\lambda_i}{T_1(\lambda_i-\omega_{12}-\omega_{23})}$. λ_i is the eigenvalue of the dressed state $|i\rangle$ $(i = a, b, c)$, giving the relative energy of the dressed state. Eq. (10) indicates that all the dressed levels $|i\rangle$ $(i = a, b, c)$ have a finite overlap with the excited state $|1\rangle$ and therefore has a nonzero dipole matrix element with ground state $|0\rangle$. As a result, the weak probe field couples the transition from state $|0\rangle$ to the three dressed states [Fig. 4(a)]. Two dark resonances arise owing to the destructive quantum interference between the three dipole-allowed transitions $|0\rangle \to |a\rangle$, $|0\rangle \to |b\rangle$ and $|0\rangle \to |c\rangle$. The double dark resonances will result in the emerging of two transparency windows and the enhancement of real part of fifth-order nonlinearity.

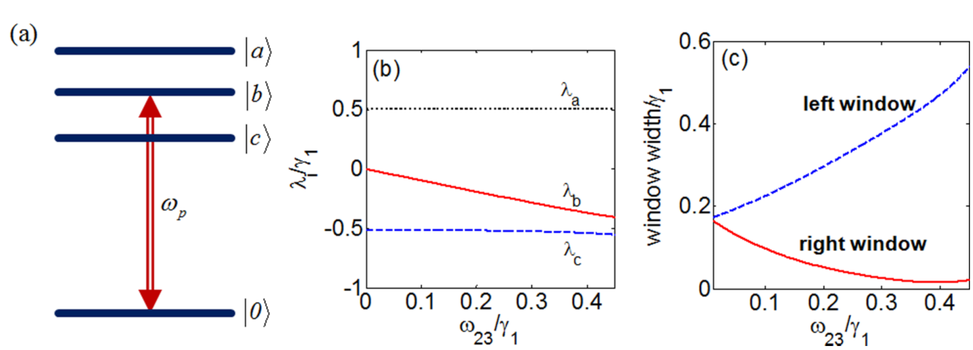

FIG. 4. (a) Dressed states of the linear TQDs under the coupling of two tunnelings T_1 and T_2. (b) The eigen energies λ_i $(i = a, b, c)$ as a function of the detuning ω_{23}. (c) The FWHM of the two transparency windows as a function of ω_{23}. Other parameters are $T_1 = 0.5$, $T_2 = 0.1$, $\omega_{12} = 0$, $\gamma_1 = 1$, $\gamma_2 = \gamma_3 = 10^{-3}\gamma_1$.

In Fig. 4(b) we show the eigen energies (λ_i, $i = a,b,c$) as a function of ω_{23}. With the increase of ω_{23}, the energy difference between λ_a and λ_b is increased, while that between λ_c and λ_b is decreased. Therefore the left and center absorption peaks become farther, while right and center absorption peaks become closer. The full width at half maximum (FWHM) of the transparency windows as a function of ω_{23} is shown in Fig. 4(c). As energy splitting ω_{23} is increasing, the right transparency window becomes narrower, while the left one becomes wider. And in the area of narrower transparency window, the dispersion profile is steeper, which enhances the real part of fifth-order nonlinearity.

III. TRIANGULAR TQDS

In this part we consider a triangular TQDs. The setup of the triangular TQDs is shown in Fig. 5(a). Three QDs are arranged triangularly, and both QD 2 and QD 3 are coupled to QD 1 with two gate electrodes. Therefore there is no tunneling between QD 2 and QD 3. Fig. 5(b) shows the energy level of the triangular TQDs. The system also consists of four levels, which are ground state $|0\rangle$, direct exciton state $|1\rangle$ and two indirect exciton states $|2\rangle$ and $|3\rangle$. Compared with linear TQDs, the main difference is that in triangular type, states $|2\rangle$ and $|3\rangle$ are coupled to state $|1\rangle$ individually and have no connection.

The Hamiltonian with the basis $\{|0\rangle, |1\rangle, |2\rangle, |3\rangle\}$ under the same approximations can be written as (assumption of $\hbar = 1$)

$$H_I = \begin{pmatrix} 0 & -\Omega_p & 0 & 0 \\ -\Omega_p & \delta_p & -T_2 & -T_3 \\ 0 & -T_2 & \delta_p - \omega_{12} & 0 \\ 0 & -T_3 & 0 & \delta_p - \omega_{13} \end{pmatrix}. \tag{11}$$

Here the Rabi frequency Ω_p and the detuning δ_p of the probe field are defined the same as above. And T_2 and T_3 are the coupling intensities of the two tunnelings, and ω_{12} and ω_{13} are the energy splittings of the excited states.

By using the same method in Sec. II, dynamical equations of atomic probability amplitudes can be obtained:

$$i\dot{a}_0 = -\Omega_p a_1, \tag{12a}$$

$$i\dot{a}_1 = -\Omega_p a_0 - T_2 a_2 - T_3 a_3 + \left(\delta_p - i\gamma_1\right) a_1, \tag{12b}$$

$$i\dot{a}_2 = -T_2 a_1 + \left(\delta_p - \omega_{12} - i\gamma_2\right) a_2, \tag{12c}$$

$$i\dot{a}_3 = -T_3 a_1 + \left(\delta_p - \omega_{13} - i\gamma_3\right) a_3, \tag{12d}$$

with $|a_0|^2 + |a_1|^2 + |a_2|^2 + |a_3|^2 = 1$. And $\gamma_i = \frac{1}{2}\Gamma_{i0} + \gamma_{i0}^d$ $(i = 1-3)$ is the typical effective decay rate, contributed by the radiative decay rate Γ_{i0} and the pure dephasing rate γ_{i0}^d.

The probe susceptibility can be expressed by Eq. (6), where χ is independent of Γ and V. Using a similar approach to that shown in Sec. II, χ can be derived:

$$\chi = \frac{1}{\Gamma_1 - \frac{T_2{}^2}{\Gamma_2} - \frac{T_3{}^2}{\Gamma_3}} \cdot \frac{1}{1 + \frac{\Omega_p{}^2}{\left|\Gamma_1 - \frac{T_2{}^2}{\Gamma_2} - \frac{T_3{}^2}{\Gamma_3}\right|^2}\left(1 + \frac{T_2{}^2}{|\Gamma_2|^2} + \frac{T_3{}^2}{|\Gamma_3|^2}\right)}, \tag{13}$$

where $\Gamma_1 = \delta_p - i\gamma_1$, $\Gamma_2 = \delta_p - \omega_{12} - i\gamma_2$, $\Gamma_3 = \delta_p - \omega_{13} - i\gamma_3$. Using the Maclaurin formula and neglecting the higher-order smaller terms, then χ can be expanded into the fourth-order of Ω_p, as expressed by Eq. (8). And $\chi^{(1)}$, $\chi^{(3)}$ and $\chi^{(5)}$ correspond to the first-order linear, the third-order nonlinear and the fifth-order nonlinear parts of the susceptibility, respectively, and the expression of them are

$$\chi^{(1)} = \frac{1}{\Gamma_1 - \frac{T_2{}^2}{\Gamma_2} - \frac{T_3{}^2}{\Gamma_3}}, \tag{14a}$$

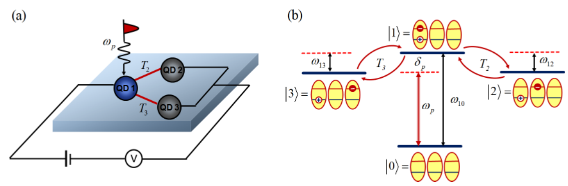

FIG. 5. (a) The schematic of the setup for triangular $TQDs$. (b) The schematic of the energy level for triangular TQDs.

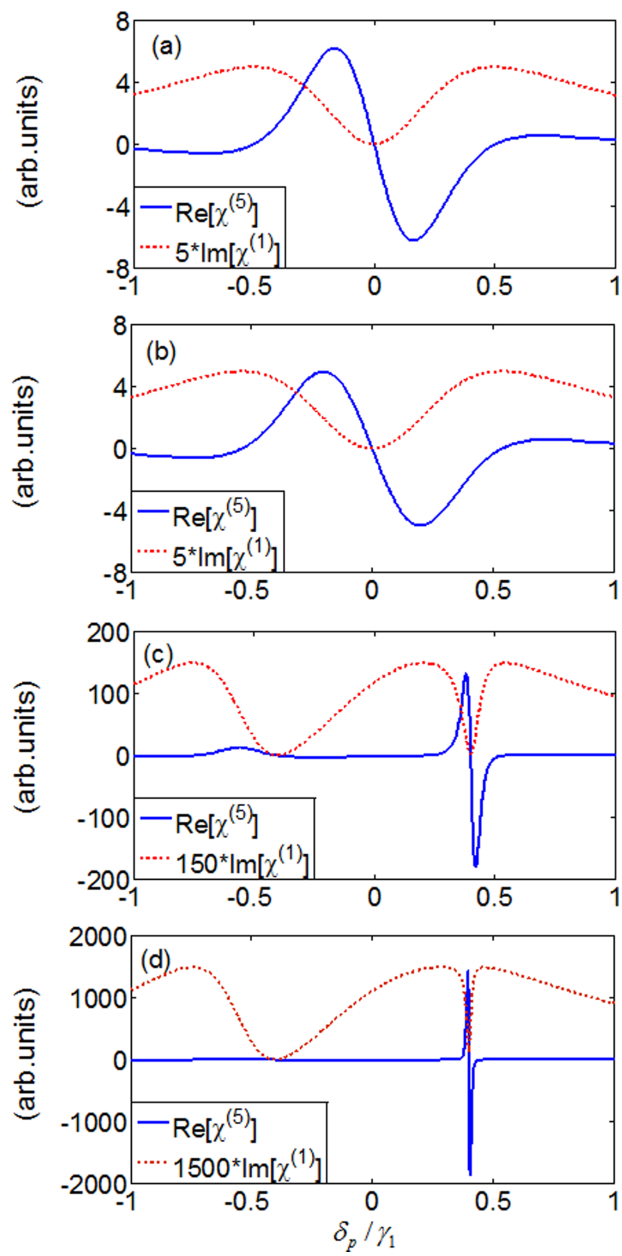

FIG. 6. Variation of the imaginary part of the linear susceptibility Im[$\chi^{(1)}$] (dotted line) and the real part of fifth-order nonlinearity Re[$\chi^{(5)}$] (solid line) as a function of probe detuning δ_p. (a) $T_3 = 0$, $\omega_{12} = \omega_{13} = 0$. (b) $T_3 = 0.2$, $\omega_{12} = \omega_{13} = 0$. (c) $T_3 = 0.2$, $-\omega_{12} = \omega_{13} = 0.4$. (d) $T_3 = 0.1$, $-\omega_{12} = \omega_{13} = 0.4$. Other parameters are $T_2 = 0.5$, $\gamma_1 = 1$, $\gamma_2 = \gamma_3 = 10^{-3}\gamma_1$.

$$\chi^{(3)} = -\frac{1}{\Gamma_1 - \frac{T_2^2}{\Gamma_2} - \frac{T_3^2}{\Gamma_3}} \cdot \frac{1}{\left|\Gamma_1 - \frac{T_2^2}{\Gamma_2} - \frac{T_3^2}{\Gamma_3}\right|^2} \cdot \left(1 + \frac{T_2^2}{|\Gamma_2|^2} + \frac{T_3^2}{|\Gamma_3|^2}\right). \tag{14b}$$

$$\chi^{(5)} = \frac{1}{\Gamma_1 - \frac{T_2^2}{\Gamma_2} - \frac{T_3^2}{\Gamma_3}} \cdot \frac{1}{\left|\Gamma_1 - \frac{T_2^2}{\Gamma_2} - \frac{T_3^2}{\Gamma_3}\right|^4} \cdot \left(1 + \frac{T_2^2}{|\Gamma_2|^2} + \frac{T_3^2}{|\Gamma_3|^2}\right)^2. \tag{14c}$$

According to Eqs. (14a) and (14c), we show the imaginary part of the linear susceptibility Im[$\chi^{(1)}$] (dotted line) and the real part of fifth-order nonlinearity Re[$\chi^{(5)}$] (solid line) as a function of δ_p in Fig. 6. First, with only one tunneling T_2, the system turns to be to a DQDs and the result is the same with that of in Fig. 2(a) [Fig. 6(a)]. From the linear absorption spectrum we can acquire one transparency window, within which the fifth-order susceptibility is small. We then apply both tunnelings T_2 and T_3, and a triangular TQDs is formed. When both the energy splittings are zero ($\omega_{12} = \omega_{13} = 0$), there is still one transparency window accomplished by smaller fifth-order susceptibility, as shown in Fig. 6(b).

Then we change the value of the energy splittings ($\omega_{12} \neq \omega_{13}$) and show the results in Fig. 6(c). In this case two transparency windows show up, one is wide on the left, while the other is narrow on the right. Meanwhile Re[$\chi^{(5)}$] is about 20 times the magnitude of that in DQDs. Keep the energy splittings unchanged and decrease the tunneling T_3, the transparency window on the right becomes even narrower. And within the narrower transparency window, Re[$\chi^{(5)}$] is significantly enhanced by about three orders of magnitude compared with DQDs [Fig. 6(d)]. Therefore giant fifth-order nonlinearity with reduced linear absorption can be obtained in the triangular TQDs, and this is useful for nonlinear applications at low light level.

Then we expand Eq. (14c) and separate it into two parts, one is denoted as F_1, which is proportional to the product of $\sum_0^2 |\Gamma_2|^{4-2n} |\Gamma_3|^{2n} T_2^{2n} T_3^{4-2n}$, and the other is denoted as F_2, which is independent of the product. We plot both the term Re[F_1] and Re[$\chi^{(5)}$] as a function of δ_p in Fig. 7 for comparison. From the figure one can see that the profile of Re[$\chi^{(5)}$] is nearly coincident with Re[F_1]. So the giant enhancement of Re[$\chi^{(5)}$] is originates from two tunneling couplings T_2 and T_3.

In the following, we explain the corresponding results under the dressed state picture, and expressions of dressed state $|i\rangle$ $(i = a, b, c)$ of the triangular TQDs is given by

$$|i\rangle = \cos\theta\cos\varphi\,|1\rangle + \cos\theta\sin\varphi\,|2\rangle + \sin\theta\,|3\rangle\,,\ (i = a, b, c) \tag{15}$$

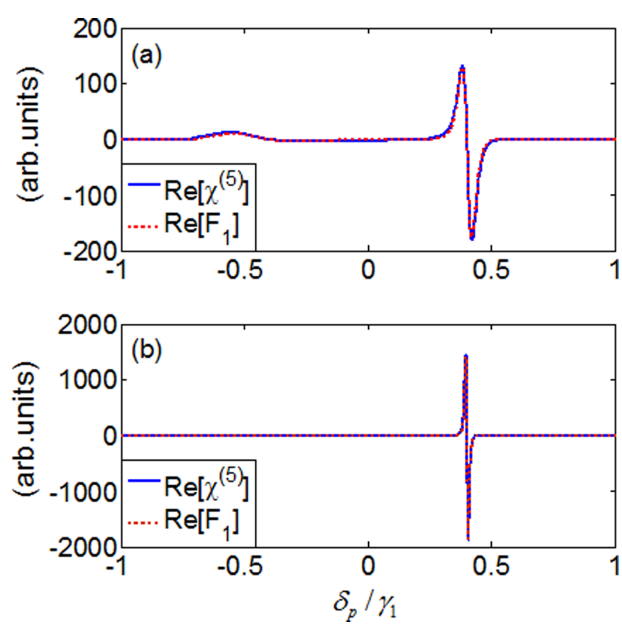

FIG. 7. Variation of Re[F_1] (dotted line) and Re[$\chi^{(5)}$] (solid line) as a function of the probe detuning δ_p. (a) $T_3 = 0.2$, (b) $T_3 = 0.1$. Other parameters are $T_2 = 0.5$, $-\omega_{12} = \omega_{13} = 0.4$, $\gamma_1 = 1$, $\gamma_2 = \gamma_3 = 10^{-3}\gamma_1$.

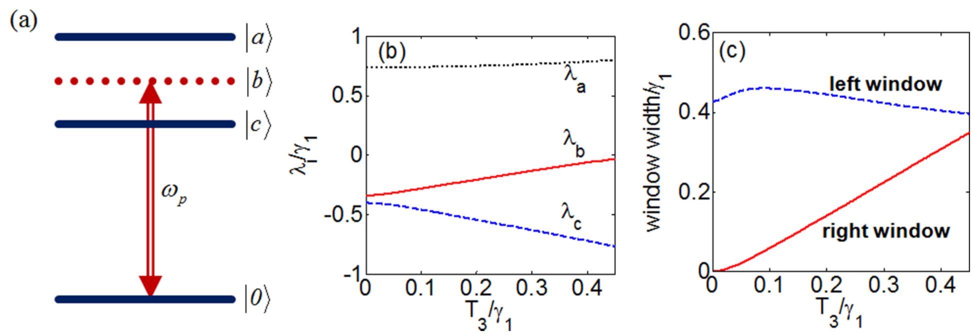

FIG. 8. (a) Dressed states of the triangular TQDs under the coupling of two tunnelings T_2 and T_3. For $\omega_{12}=\omega_{13}$, only dressed state $|a\rangle$ and $|c\rangle$ are coupled to the state $|0\rangle$. For $\omega_{12}\neq\omega_{13}$, all three dressed state $|a\rangle$, $|b\rangle$ and $|c\rangle$ are coupled to the state $|0\rangle$. (b) The eigen energies λ_i $(i=a,b,c)$ as a function of T_3. (c) The FWHM of the two transparency windows as a function of T_3. Other parameters are $T_2=0.5$, $-\omega_{12}=\omega_{13}=0.4,\gamma_1=1$, $\gamma_2=\gamma_3=10^{-3}\gamma_1$.

where $\tan\varphi=-\frac{T_2}{\omega_{12}+\lambda_i}$ and $\tan\theta=\frac{(\omega_{12}+\lambda_i)T_3}{(\omega_{13}+\lambda_i)\sqrt{T_2{}^2+(\omega_{12}+\lambda_i)^2}}$. λ_i is the eigenvalue of the dressed state $|i\rangle$ $(i=a,b,c)$, giving the relative energy of the three dressed state. Therefore the weak probe field couples the transition from state $|0\rangle$ to the dressed state $|i\rangle$ [Fig. 8(a)]. In the case of $\omega_{12}=\omega_{13}$, only the dressed state $|a\rangle$ and $|c\rangle$ contain an admixture of $|1\rangle$. So there is only one dark state, which results from quantum interference between the two transitions $|0\rangle\rightarrow|a\rangle$ and $|0\rangle\rightarrow|c\rangle$. While in the case of $\omega_{12}\neq\omega_{13}$, all the dressed levels $|a\rangle$, $|b\rangle$ and $|c\rangle$ have a finite overlap with the excited state $|1\rangle$ and has a nonzero dipole matrix element with ground state $|0\rangle$. Therefore quantum interference between transitions $|0\rangle\rightarrow|a\rangle$, $|0\rangle\rightarrow|b\rangle$ and $|0\rangle\rightarrow|c\rangle$ can result in dounle dark resonances, which are responsible for the emergency of two transparency windows and the enhancement of real part of fifth-order nonlinearity.

Now we can interpret the dependence of fifth-order nonlinearity on the tunneling T_3. According to Eq. (15), we plot the eigen energies and FWHM of the transparency windows of the triangular TQDs as a function of T_3 in Figs. 8(b) and 8(c), respectively. As can be seen, with decreasing tunneling T_3, the left transparency window changes small, while the right transparency window becomes narrower. Within the narrower transparency window, the probe dispersion is steeper, and as a consequence $\mathrm{Re}[\chi^{(5)}]$ is greatly enhanced.

IV. CONCLUSIONS

It is demonstrated that the giant enhancement of the fifth-order nonlinearity can be acquired in both linear and triangular TQDs via two tunneling couplings. Compared with DQDs, the fifth-order nonlinearity of TQDs is increased to three orders of magnitude, and simultaneously the absorption vanishes with proper parameters. An analytical expression indicates that it is the two tunnelings that give rise to enhanced fifth-order nonlinearity. The dressed states of both configurations of TQDs are also investigated to understand the dependence of fifth-order nonlinearity on the tunneling parameters. The ability to create the giant fifth-order nonlinearity could prove useful for applications in quantum information processing, such as multiwave mixing and optical solitons.

ACKNOWLEDGMENTS

This work is supported by the financial support from the National Natural Science Foundation of China (Grant Nos. 11304308 and 61176046), the National Basic Research Program of China (Grant Nos. 2013CB933300), the International Science Technology Cooperation Program of China (No. 2013DFR00730), and the Hundred Talents Program of Chinese Academy of Sciences, and Jilin Provincial Natural Science Foundation (Grant Nos. 20140101203JC).

[1] N. O. Boyd R. W., 3rd edition (Academic Press) 2008, Chapt. 3.
[2] S. E. Harris and L. V. Hau, Phys. Rev. Lett. **82**, 4611 (1999).
[3] H. Kang and Y. Zhu, Phys. Rev. Lett. **91**, 093601 (2003).
[4] H. Schmidt and A. Imamoglu, Opt. Lett. **21**, 1936 (1996).
[5] H. Wang, D. Goorskey, and M. Xiao, Phys. Rev. Lett. **87**, 073601 (2001).
[6] A. B. Matsko, I. Novikova, G. R. Welch, and M. S. Zubairy, Opt. Lett. **28**, 96 (2003).
[7] S. Rebić, D. Vitali, C. Ottaviani, P. Tombesi, M. Artoni, F. Cataliotti, and R. Corbalán, Phys. Rev. A **70**, 032317 (2004).
[8] Y. Niu, S. Gong, R. Li, Z. Xu, and X. Liang, Opt. Lett. **30**, 3371 (2005).
[9] S. Li, X. Yang, X. Cao, C. Zhang, C. Xie, and H. Wang, Phys. Rev. Lett. **101**, 073602 (2008).
[10] S. E. Harris, Physics Today **50**, 36 (1997).
[11] S. Saito and I. Ohmine, Phys. Rev. Lett. **88**, 207401 (2002).
[12] L. J. Kaufman, J. Heo, L. D. Ziegler, and G. R. Fleming, Phys. Rev. Lett. **88**, 207402 (2002).
[13] Y. Zhang, U. Khadka, B. Anderson, and M. Xiao, Phys. Rev. Lett. **102**, 013601 (2009).
[14] K. Dolgaleva, H. Shin, and R. W. Boyd, Phys. Rev. Lett. **103**, 113902 (2009).
[15] A. G. Joel and J. G. Daniel, EPL (Europhysics Letters) **98**, 24001 (2012).
[16] Z. Wu, Y. Zhang, C. Yuan, F. Wen, H. Zheng, Y. Zhang, and M. Xiao, Phys. Rev. A **88**, 063828 (2013).
[17] W. X. Yang, A. X. Chen, R. K. Lee, and Y. Wu, Phys. Rev. A **84**, 013835 (2011).
[18] E. L. Falcão-Filho, C. B. de Araújo, G. Boudebs, H. Leblond, and V. Skarka, Phys. Rev. Lett. **110**, 013901 (2013).
[19] Á. Paredes, D. Feijoo, and H. Michinel, Phys. Rev. Lett. **112**, 173901 (2014).
[20] L. Wang, A. Rastelli, S. Kiravittaya, M. Benyoucef, and O. G. Schmidt, Adv. Mater. **21**, 2601 (2009).
[21] A. Boyer de la Giroday, N. Sköld, R. M. Stevenson, I. Farrer, D. A. Ritchie, and A. J. Shields, Phys. Rev. Lett. **106**, 216802 (2011).
[22] D. Kim, S. G. Carter, A. Greilich, A. S. Bracker, and D. Gammon, Nat. Phys. **7**, 223 (2011).
[23] K. Müller, A. Bechtold, C. Ruppert, M. Zecherle, G. Reithmaier, M. Bichler, H. J. Krenner, G. Abstreiter, A. W. Holleitner, J. M. Villas-Boas, M. Betz, and J. J. Finley, Phys. Rev. Lett. **108**, 197402 (2012).
[24] K. M. Weiss, J. M. Elzerman, Y. L. Delley, J. Miguel-Sanchez, and A. Imamoğlu, Phys. Rev. Lett. **109**, 107401 (2012).
[25] C. H. Yuan and K. D. Zhu, Appl. Phys. Lett. **89**, 052115 (2006).
[26] M. T. Cheng, X. S. Ma, Y. Q. Luo, P. Z. Wang, and G. X. Zhao, Appl. Phys. Lett. **99**, 223509 (2011).
[27] S. C. Tian, C. Z. Tong, C. L. Wang, L. J. Wang, H. Wu, E. B. Xing, Y. Q. Ning, and L. J. Wang, Opt. Commun. **312**, 296 (2014).
[28] E. Voutsinas, A. F. Terzis, and E. Paspalakis, Phy. Lett. A **378**, 219 (2014).
[29] Y. D. Peng, A. H. Yang, D. H. Li, H. Zhang, Y. P. Niu, and S. Q. Gong, Laser Phys. Lett. **11**, 065201 (2014).
[30] Q. Xie, A. Madhukar, P. Chen, and N. P. Kobayashi, Phys. Rev. Lett. **75**, 2542 (1995).
[31] R. Songmuang, S. Kiravittaya, and O. G. Schmidt, Appl. Phys. Lett. **82**, 2892 (2003).
[32] G. Rainò, A. Salhi, V. Tasco, M. De Vittorio, A. Passaseo, R. Cingolani, M. De Giorgi, E. Luna, and A. Trampert, J. Appl. Phys. **103**, 096107 (2008).
[33] C. Y. Hsieh, Y. P. Shim, M. Korkusinski, and P. Hawrylak, Rep. Prog. Phys. **75**, 114501 (2012).
[34] R. Yu, J. Li, C. Ding, and X. Yang, Phy. Lett. A **375**, 2738 (2011).
[35] S. C. Tian, C. Z. Tong, R. G. Wan, Y. Q. Ning, and L. J. Wang, arXiv:1310.4599 (2013).
[36] S. C. Tian, R. G. Wan, C. Z. Tong, Y. Q. Ning, L. Qin, and Y. Liu, J. Phys. B: At. Mol. Opt. Phys. **47**, 155503 (2014).
[37] M. Sahrai, M. R. Mehmannavaz, and H. Sattari, Appl. Opt. **53**, 2375 (2014).
[38] S. C. Tian, R. G. Wan, C. Z. Tong, Y. Q. Ning, L. Qin, and Y. Liu, J. Opt. Soc. Am. B **31**, 1436 (2014).
[39] S. C. Tian, R. G. Wan, C. Z. Tong, and Y. Q. Ning, J. Opt. Soc. Am. B **31**, 2681 (2014).
[40] Y. D. Peng, A. H. Yang, B. Chen, Y. Xu, and X. J. Hu, J. Opt. Soc. Am. B **31**, 2188 (2014).
[41] G. S. Agarwal, *Quantum Optics* (Springer-Verlag, Berlin, 1974).
[42] S. M. Barnett and P. M. Radmore, *Methods in Theoretical Quantum Optics* (Oxford University Press, Oxford, 1997).
[43] J. Kim, S. L. Chuang, P. C. Ku, and C. J. Chang-Hasnain, J. Phys.: Condens. Matter **16**, S3727 (2004).